Journal of the Korean Chemical Society
2012, *Vol. 56, No. 1*
Printed in the Republic of Korea
http://dx.doi.org/10.5012/jkcs.2012.56.1.014

Density Functional Theory Study of Competitive Reaction Pathways of Ti^+ with Fluorinated Acetone in the Gas Phase

Kiryong Hong and Tae Kyu Kim*
*Department of Chemistry and Chemistry Institute of Functional Materials, Pusan National University, Busan 609-735, Korea. *E-mail: tkkim@pusan.ac.kr*
(Received November 14, 2011; Accepted November 25, 2011)

ABSTRACT. We investigate the doublet and quartet potential energy surfaces associated with the gas-phase reaction between Ti^+ and CF_3COCH_3 for two plausible reaction pathways, TiF_2^+ and TiO^+ formation pathways by using the density functional theory (DFT) method. The molecular structures of intermediates and transition states involved in these reaction pathways are optimized at the DFT level by using the PBE0 functional. All transition states are identified by using the intrinsic reaction coordinate (IRC) method, and the resulting reaction coordinates describe how Ti^+ activates CF_3COCH_3 and produces TiF_2^+ and TiO^+ as products. On the basis of presented results, we propose the most favorable reaction pathway in the reaction between Ti^+ and CF_3COCH_3.

Key words: Ti^+, Density functional theory, Ion-molecule reaction

INTRODUCTION

Recent studies of the chemical reactions between transition metal ions and various organic molecules in the gas phase have yielded important insights, not only into the catalytic activity of transition metal ions, but into the reaction mechanisms and the structures of complexes that are present in many important organometallic reactions.[1-4] For this purpose, there have been many theoretical studies aiming at explaining reaction mechanisms of the first-row transition-metal ions with simple organic molecules.[5-10] Among these studies, the reactions of metal cations with acetone (ACT) have been extensively investigated and reaction pathways appear to be varied depending on the metal ion involved.[8-10] Due to the strong binding ability of the early transition metal ions such as Ti^+ and Sc^+, the reaction of Ti^+ with acetone gives the reaction products of TiO^+ and CH_2CHCH_3. Recently it has been shown that density functional theory (DFT) has been used to study the oxidation pathway of acetone with Ti^+ and the resulting reaction coordinates describe how Ti^+ activates the C=O bond of CH_3COCH_3 and yields TiO^+ and CH_2CHCH_3 as products.[8] This theoretical study can explain experimental findings and give a deeper understanding to the reaction mechanism.[8]

When H atoms in CH_3COCH_3 are substituted by highly electronegative F atoms, it is expected that reaction pathways are altered significantly due to the strong binding affinity of Ti^+ ion to the F atoms. Therefore the reaction of Ti^+ with CF_3COCH_3 (1,1,1-trifluoroacetone, TFA) provides a good model system to examine the influence of fluorine substituents on the chemical reactivity of Ti^+ with acetone. Our recent experimental results[11] show that both TiF_2^+ and TiO^+ ions can be produced in the reaction of Ti^+ and TFA. This finding implies that the fluorine atom substitution can significantly alter the reaction pathways and related energetics in the reaction between Ti^+ and TFA. Here we have investigated reaction pathways and relevant potential energy surfaces (PES) of reactions between Ti^+ and TFA in the gas phase using the DFT method. Based on calculated results, we propose the most favorable reaction pathway in the reaction between Ti^+ and TFA.

CALCULATION METHODS

The molecular geometries and harmonic vibrational frequencies were calculated by using DFT. The PBE0 (Hybrid, 25% of the exact exchange energy) functional[12,13] was used for the reaction of Ti^+ with TFA. The structures of all the reactants, products, intermediates, and transition states involved in the title reaction were fully optimized at the PBE0/6-311++G(d,p) levels of theory. Considering the possible spin-orbit coupling interactions that allow an intersystem crossing from the quartet to the doublet in the course of Ti^+ with TFA, both the doublet and quartet PESs for reaction of Ti^+ with TFA were searched.[8-10] The calculation details have been described in our previous work.[8,10] Once we found the association complexes between Ti^+ and

TFA, we verified transition state to connect a desired pair of minima by tracing the intrinsic reaction coordinate (IRC).[14] Frequency calculations were performed at the same level to identify the stationary points and to estimate zero-point energy (ZPE) corrections that are applied to all reported energies. Natural bond orbital (NBO) analysis was also carried out for some important stationary points to gain electron configurations and bonding properties. All DFT calculations were performed using the GAUSSIAN 03 package.[15]

RESULTS AND DISCUSSION

Based on our experimental results for ion-molecule reaction between Ti^+ and TFA, here we estimated and performed electronic structure calculations for two plausible reaction pathways as followings:

$$Ti^+ + CF_3COCH_3 \rightarrow TiO^+ + F_2C=CFCH_3 \quad (1)$$
$$\rightarrow TiF_2^+ + FCOCHCH_2 \quad (2)$$

Unlike the Ti^+ + ACT reaction, in which only TiO^+ ions are generated by insertion of Ti^+ ions into the C=O bond of ACT molecules,[10] both TiF_2^+ and TiO^+ ions are observed in the reaction of Ti^+ and TFA.[11] The optimized geometries of the stationary points in both doublet and quartet states for TiO^+ and TiF_2^+ formation reaction pathways are depicted in *Figs*. 1 and 2, respectively. *Figs*. 3(A) and 3(B) show the relevant PES along with the TiO^+ and TiF_2^+ formation reaction pathways, respectively. In all cases, the superscript denotes the spin multiplicity. In typical ion-molecule experimental condition,[10] it is highly unlikely that the radical form of isomer can be generated. Therefore we described the most stable species as shown below. In this paper, we used the notations of IM*n* and TS*nm* for the intermediate *n* and the transition state between IM*n* and IM*m*, respectively. First, the excited state of $Ti^+(^2F)$ was calculated to lie 15.9 kcal·mol^{-1} above the ground state of $Ti^+(^4F)$ at the PBE0/6-311++G(d,p) levels of theory, which was in well agreement with the experimental value. This demonstrates the accuracy of our calculated results.[8]

To form a stable association complex, initially a Ti^+ ion attacks the electron-rich oxygen of the TFA. ^{2}IM1 and ^{4}IM1 complexes are calculated to be more stable by 30.5 kcal/mol (^{4}IM1) and 45.2 kcal/mol (^{2}IM1), respectively, than the isolated reactants. The complex $^4IM_1$ has a nearly linear binding of Ti^+-O-C (170.2°), remarkably different from the bent geometry of the Ni^+-CH_3COCH_3 association complex ($\angle Ni^+$-O-C=138.8°), which produces $Ni^+CO+C_2H_6$ fragments.[9] Once the association complexes formed, the next step carries the association complex to the fluoride-containing species IM2 via transition state TS12. As shown in *Fig*. 1, this process is strictly analogous to the fluorine atom-migration for HMg^+-$OCHCH_2$ from Mg^+-$OCHCH_3$, in which the transition state has a five-membered structure.[16] It could be assumed that intersystem crossing (ISC) takes place between the ground spin state (^{4}F) and the doublet spin state (^{2}F) reaction pathways during process between TS12 and IM2. Similarly, intersystem crossing between the doublet and quartet spin states also has been observed in the gas phase ion-molecule reactions of Ti^+ with CH_4, CH_3OCH_3, and CH_3CHO.[5,7,17] After this intersystem crossing, two alternative pathways can be initiated along the reaction coordinate.

The PES for TiO^+ formation pathway is shown in *Fig*. 3(A). Following the TiO^+ formation pathway, the insertion of Ti^+ into the C1=O bond of TFA to produce the IM3 via ^{2}TS23 and ^{4}TS23 with a process barrier of 38.3 and 66.0 kcal·mol^{-1}, respectively. The bond distance of C1-O in TFA is substantially elongated in TS23 compared to those in IM2. The reaction barrier between ^{2}IM2 and ^{2}TS23 constituted the largest barrier on the doublet PES of TiO^+ formation pathway, suggesting that the Ti^+ insertion into C1=O bond is the rate-determining step of this pathway. After IM3, an electrostatic complex (IM4) between TiO^+ and CF_2CFCH_3, the direct precursor of products in this pathway, is produced by the intra-rotation of Ti^+-F bond. The structure of IM4 is well characterized by five-membered ring structure. The dissociation of the (CF_2CHCH_3)-TiO^+ bond of IM4 gives rise to $TiO^+ + CF_2CFCH_3$ and the TiO^+ pathway is computed to be exothermic by 38.5 kcal·mol^{-1} for $TiO^+(^2\Delta) + CF_2CFCH_3$ and 46.5 kcal·mol^{-1} endothermic for producing $TiO^+(^4\Delta) + CF_2CFCH_3$.

Another reaction pathway is TiF_2^+ formation pathway to account for final products of $TiF_2^+ + FCOCHCH_2$. The PES for this pathway is displayed in *Fig*. 3(B). Like the TiO^+ formation pathway, this pathway also starts from ^{4}IM1, passes through ISC and produces ^{2}IM2. Then, the C1-O-Ti^+ scissor vibration in IM2 transfers the second F atom to the metal center to form complex IM5 through ^{2}TS25 or ^{4}TS25. The five-membered doublet transition state ^{2}TS25 (E_{rel} = -82.0 kcal·mol^{-1}) is more stable than ^{4}TS25. It is interesting to note that both ^{4}IM5 and ^{2}IM5 indeed have an almost identical stability (^{2}IM5 is 0.2 kcal·mol^{-1} stable than ^{4}IM5) as well as same structure whose Ti^+-O bond is largely weakened (R_{CO}=1.957-1.960Å): thus effectively isolating the TiF_2^+ from the association complex. The forward intermediate from IM5 is IM6, which involves a

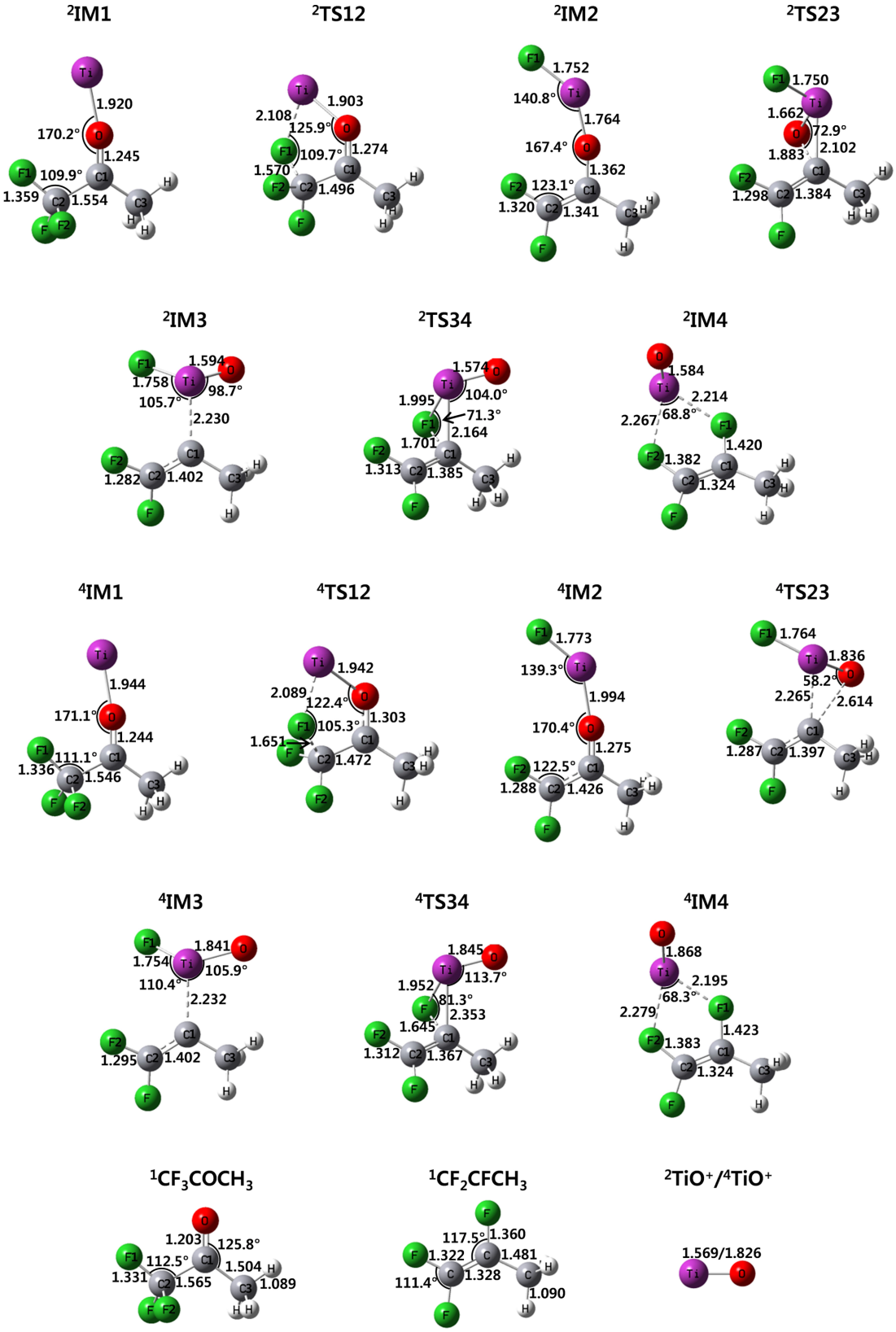

***Fig.* 1.** Optimized geometrical parameters (bond lengths in Å and angles in degrees) for the stationary points found in both doublet and quartet electronic states for TiO^+ formation pathway at the PBE0/6-311++G(d,p) level.

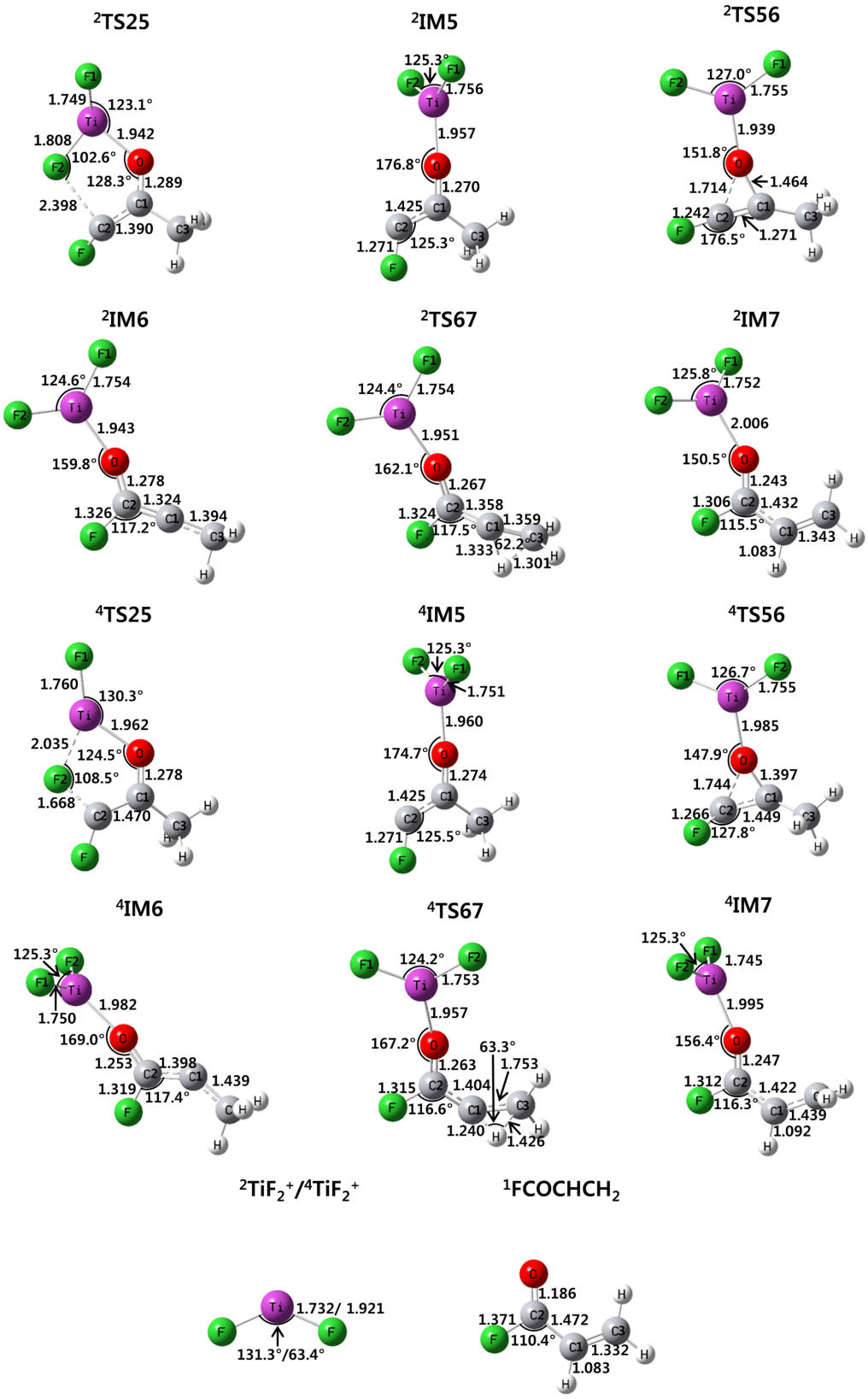

***Fig.* 2.** Optimized geometrical parameters (bond lengths in Å and angles in degrees) for the stationary points found in both doublet and quartet electronic states for TiF_2^+ formation pathway at the PBE0/6-311++G(d,p) level.

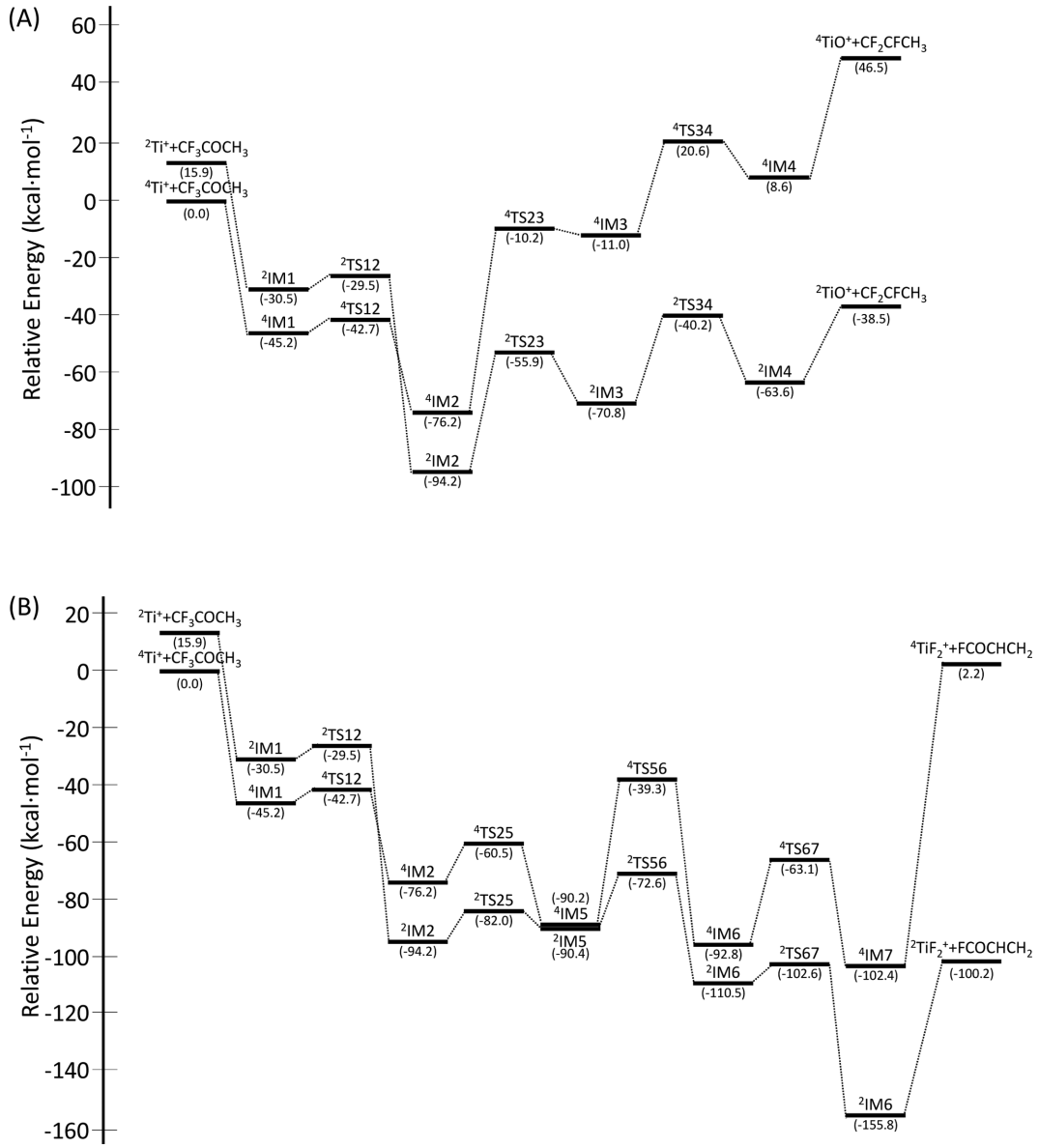

***Fig.* 3.** Potential energy diagrams along TiO^+ (A) and TiF_2^+ (B) formation pathways.

three-membered ring ^{2}TS56 and ^{4}TS56 with a barrier of 17.8 and 50.9 kcal·mol^{-1}, respectively. An interaction takes place between O and both C1 and C2 in the TS56. The energy of ^{2}IM6 is 10.3 kcal·mol^{-1} lower than that of the entrance channel. The H atom then migrates into C1 from C3 atoms, forming electrostatic complex, IM7 between TiF_2^+ and $FCOCHCH_2$, the direct precursor of products in the TiF_2^+ formation pathway (TiF_2^+ + $FCOCHCH_2$). Although the reaction barrier between IM7 (E_{rel} = -155.8 kcal·mol^{-1}) and products represents the deepest barrier along the doublet surface of the TiF_2^+ formation pathway, this effect can be attributed to the strong stabilization of both the constituent entities ($^2TiF_2^+$ and $FCOCHCH_2$). Therefore, the actual rate determining step in this pathway exists between IM5 and TS56, which gives the reaction barrier of 17.8 kcal·mol^{-1}. Fragmentation of the ($FCOCHCH_2$)-TiF_2^+ bond of IM7 gives rise to the products of this pathway and the overall reaction energy of the $^4Ti^+$+CF_3COCH_3 $\rightarrow$$^2TiF_2^+$ + $FCOCHCH_2$ is calculated to be -100.2 kcal·mol^{-1}.

In summary, a comparison between the values of the relative energies of the highest TSs for both reaction pathways shows that ^{2}TS23 (-38.3 kcal·mol^{-1}) has a larger value than ^{2}TS56 (-17.8 kcal·mol^{-1}), suggesting that TiF_2^+ ions are primary reaction products. However, TiF_2^+ formation

pathway is rather complex than TiO^+ formation channel in terms of the number of involved reaction steps. Therefore two reaction pathways can be considered as competitive pathways, which is well in agreement with experimental findings. These reaction pathways account for how Ti^+ activates CF_3COCH_3 in the gas phase and subsequently produces the competitive reaction products in detail.

Acknowledgements. This work was supported by for two years by Pusan National University Research Grant.

REFERENCES

1. Roithová, J.; Schröder, D. *Chem. Rev.* **2010**, *110*, 1170.
2. Garvey, J. F.; Peifer, W. R.; Coolbaugh, M. T. *Acc. Chem. Res.* **1991**, *24*, 48.
3. Koo, Y.-M.; Kim, T. K.; Jung, D. W.; Jung, K.-W. *J. Phys. Chem. A* **2006**, *248*, 810.
4. Paul, D.; Hong, K.; Kim, T. K.; Jung, K.-W. *Bull. Korean Chem. Soc.* **2010**, *31*, 271.
5. Wang, Y.-C.; Liu, Z.-Y.; Geng, Z.-Y.; Yang, X.-Y. *Chem. Phys. Lett.* **2006**, *427*, 271.
6. Zhao, L.; Guo, W.; Zhang, R.; Wu, S.; Lu, X. *Chem. Phys. Chem*. **2006**, *7*, 1345.
7. Ding, N.; Zhang, S.; Chen, X. *Chem. Phys. Lett.* **2008**, *459*, 33.
8. Kim, J.; Kim, T. K.; Ihee, H. *J. Phys. Chem. A* **2009**, *113*, 11382.
9. Chen, X.; Guo, W.; Zhao, L.; Fu, Q. *Chem. Phys. Lett.* **2006**, *432*, 27.
10. Koo, Y.-M.; Hong, K.; Kim, T. K.; Jung, K.-W. *Bull. Korean Chem. Soc.* **2010**, *31*, 953.
11. Paul, D.; Hong, K.; Jung, K. W.; Kim, T. K. *Chem. Phys. Lett.* submitted.
12. Adamo, C.; Barone, V. *J. Chem. Phys.* **1999**, *110*, 6158.
13. Ernzerhof, M.; Scuseria, G. E. *J. Chem. Phys.* **1999**, *110*, 5029.
14. Gonzalez, C.; Schlegel, H. B. *J. Phys. Chem.* **1990**, *94*, 5523.
15. Frisch, M. J., *et al*. *Gaussian*, Revision E.01.; Gaussian, Inc.: Wallingford, CT, 2004.
16. Liu, H.-C; Wang, C.-S. Guo, W.; Wu, Y.-D.; Yang, S. *J. Am. Chem. Soc.* **2002**, *124*, 3794.
17. Sunderlin, L. S.; Armentrout, P. B. *J. Phys. Chem.* **1988**, *92*, 1209.